

# The free fall in three physics theories

E. Luna-Hernández\*, J. Bernal and L. E. Ramón

Universidad Juárez Autónoma de Tabasco, División Académica de Ciencias Básicas,  
86690, Cunduacán, Tabasco.

\*e-mail: edgarlhdez1@gmail.com

Received 25 February 2023; accepted 22 August 2023

This paper explores the interplay between Classical Mechanics, Relativistic Mechanics, and Quantum Mechanics through an analysis of the free fall phenomenon. We investigate the probability density functions and corresponding plots in each theory, alongside calculating the expected values of position and momentum. By observing the behavior of these results as they approach the classical limit, we confirm the hypothesis that these theories can be connected through their probability density functions. Furthermore, we discuss the validity of the correspondence principle in Quantum Mechanics, while also examining, in a non-rigorous manner, the validity of the weak equivalence principle within each of the aforementioned theories.

**Keywords:** Asymptotic quantum mechanics; correspondence principle; probability density; relativistic form of Newton’s second law; weak equivalence principle.

DOI: <https://doi.org/10.31349/RevMexFisE.21.010214>

## 1. Introduction

In 1990, the first Physics forum was held in Tabasco<sup>i</sup>, with the participation of Marcos Moshinsky<sup>ii</sup>, who gave one of his famous outreach talks “Las Tres Caras de la Mecánica” from which the authors of the present work were inspired. In such talks, Moshinsky mentioned that there are various theories in Physics that are circumscribed to the different scales of speeds  $v$  and actions  $S$ , in comparison with the speed of light in the vacuum  $c$  and Planck’s constant  $h$  respectively. To understand this, the diagram shown in Fig. 1 graphically illustrates an extension of such idea, adding a new description axis in which General Relativity appears. This diagram is interpreted as follows:

- When velocities are small compared to the speed of light ( $c$ ) and actions are large compared to the Planck constant ( $h$ ), Classical Mechanics provides a valid description.
- In the regime of large velocities compared to  $c$  and large actions compared to  $h$ , Relativistic Mechanics or Special Relativity is applicable.
- When velocities are small compared to  $c$  and actions are on the order of  $h$ , the effects of Quantum Mechanics become evident.
- At high velocities compared to  $c$  and actions on the order of  $h$ , the study pertains to Relativistic Quantum Mechanics.
- Additionally, the curvature of space-time, characterized by the Ricci scalar  $R$  derived from the Riemann Tensor, becomes relevant, giving rise to General Relativity. When  $R$  is considered null, the first four theories

described above, applicable to flat space-time, are recovered.

One of the most basic and fundamental concepts in Physics is that of free fall phenomenon, which occurs when an object is in a state of motion under the influence of gravity alone. Such phenomenon provides an ideal example to study the behavior of a particle across distinct physical approaches. In this work, we examine the free fall of a particle within three Physics theories: Classical Mechanics, Relativistic Mechanics, and Quantum Mechanics.

It is worth noting that previous studies have already explored the relationship between classical and quantum systems, with a particular focus on the quantum bouncer [2], which is a simple quantum system that mimics the behavior of a classical particle bouncing against a potential wall. In this analysis, the surface on which the particle bounces is as-

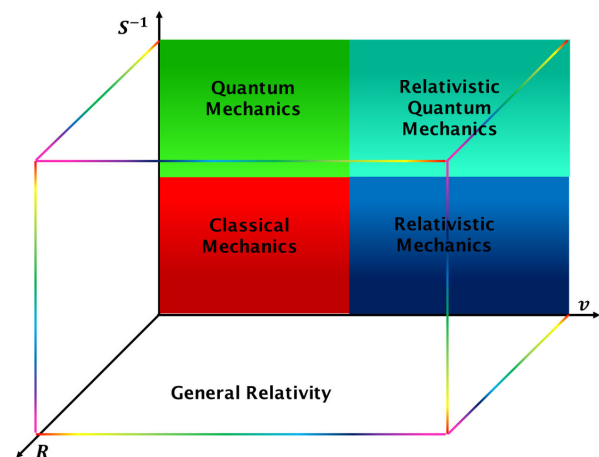


FIGURE 1. Qualitative diagram of the different theories in Physics depending on the size of the action ( $S$ ), the velocity ( $v$ ), and curvature ( $R$ ).

sumed to be ideally reflective, resulting in a perfectly elastic collision. However, the present study does not consider the rebound of the particle after collision.

We delve into the concept of classical probability density and its application to Classical Mechanics and Relativistic Mechanics, which are the main focus of this study. The analysis also confirms the Bohr-Heisenberg correspondence principle in the quantum case, which asserts that “Quantum Mechanics reproduces Classical Mechanics in the limit of large quantum numbers” [3].

We also specifically examine the independence of the mass of the particle on the probability density per unit length. While this observation can be seen as a necessary condition for the weak equivalence principle, which states that “all point-like particles fall along the same path within a gravitational field, regardless of frictional effects” based on Galileo’s pioneering ideas [4], it’s important to note that we do not provide a formal proof or verification of the principle itself for each theory addressed.

The main aim of this work is to deepen students’ understanding at the undergraduate level of these three theories by exploring their behavior in a simple and shared scenario. The example of free fall highlights both the differences and the similarities between the theories, particularly in their depiction of the probability density function.

## 2. Probability density: Concepts

The probability differential  $dP$  of a particle is defined as the product of the probability density per unit length  $\rho(y)$  and the position differential  $dy$ . This differential is proportional to the time differential  $dt$  divided by the total travel time  $T$  [5]:

$$dP = \rho(y) dy \propto \frac{dt}{T}. \quad (1)$$

Solving  $\rho(y)$ , the expression is obtained to calculate the probability density per unit length, given by the expression:

$$\rho(y) = \frac{dP}{dy} = \frac{1}{T|v(y)|}, \quad (2)$$

where  $v(y)$  is the velocity expressed in terms of the position of the particle. This probability density represents the randomly selected portion of events within a specific position interval  $dy$  when an experiment or phenomenon, such as free fall, is repeated numerous times. It is important to note that this classical definition of probability density differs mathematically from the definition in Quantum Mechanics, where it is calculated as the squared norm of the wave function  $\psi$ . The wave function provides information about the physical state of the particle within the system. In the classical context, the analog of this function would be the square root of the probability density (2). Therefore, the expression for the

probability differential is as follows:

$$dP = \rho(y) dy = \frac{1}{T|v(y)|} dy. \quad (3)$$

For the probability density definition given above to be physically valid, it must satisfy the normalization condition:

$$P(\Omega) = \int_{\Omega} dP = 1. \quad (4)$$

Then, if we consider a region  $\mathcal{A} \subset \Omega$ , where  $\Omega$  is a region at position space. So, the probability of locating the particle in such zone is calculated by:

$$P(\mathcal{A}) = \int_{\mathcal{A}} dP, \quad (5)$$

where clearly:  $0 < P(\mathcal{A}) < 1$ . Additionally, the probability density per unit momentum is defined [5]:

$$\rho(p) = \frac{dP}{dp} = \frac{1}{T|F(p)|}. \quad (6)$$

Considering  $F(p)$  as the force expressed in terms of particle momentum. Then, the probability density (6) analogously represents the portion of randomly selected events within a given momentum interval  $dp$ . The analysis related to this probability density will focus on calculating the expected values of momentum.

## 3. Expected values: Position and momentum

Given the classical probability density, it is possible to calculate the expected value, which represents the average of all possible outcomes of an experiment related to a specific observable, such as position or any other observable expressed in those terms [6]. Specifically, the expected value for position is calculated from the probability density per unit length:

$$\langle y \rangle = \int_{\Omega} \rho(y) y dy. \quad (7)$$

Similarly, the expected value for momentum is calculated from the probability density per unit momentum:

$$\langle p \rangle = \int_{\Omega} \rho(p) p dp. \quad (8)$$

Considering  $\Omega'$  as a region defined in momentum space.

The following sections explore the analysis of the free fall phenomenon, specifically focusing on the discussion of probability density associated with each theory utilized to study this phenomenon.

## 4. Classical case

Let’s consider a particle with mass  $m$  that starts falling from rest at  $t = 0$  from an initial height  $H$ . The particle is uniformly accelerated under the influence of the terrestrial gravitational field, neglecting any effects of air friction. The initial

conditions for  $v(t)$  and  $y(t)$  in this problem can be stated as follows:

$$v(0) = 0, \quad y(0) = H. \quad (9)$$

Starting from Newton's second law [7] and considering the force due to the gravitational field, it follows that the value of the acceleration is given by the terrestrial standard gravity  $g$ . Since the motion is one-dimensional and vertical, it can be analyzed using a single vector component.

By solving the corresponding differential equations using the initial condition provided in (9), we obtain the kinematic equations for the functions  $v(t)$  and  $y(t)$ :

$$v(t) = -gt, \quad (10)$$

$$y(t) = H - \frac{1}{2}gt^2. \quad (11)$$

Combining (10) and (11) gives the velocity in terms of the position  $y$ :

$$v(y) = -\sqrt{2g(H-y)}, \quad (12)$$

where the maximum velocity occurs at the instant just before the particle reaches the ground, which corresponds to when  $y \rightarrow 0$ . Evaluating (12) at this point, we can determine the maximum speed:

$$v_{\max} = -\sqrt{2gH}. \quad (13)$$

In addition, the total fall time  $T$  is obtained just at the instant in which the particle reaches the surface and coincides with its maximum velocity:

$$T_{cl} = \sqrt{\frac{2H}{g}}. \quad (14)$$

Considering the knowledge of the function  $v(y)$ , the period  $T$ , and the region of space in which the trajectory is defined, denoted as  $\Omega : 0 < y \leq H$ , we can calculate the probability density per unit length.

To derive the expression, we substitute (12) and (14) into (2), resulting in the following expression:

$$\rho_{cl}(y) = \frac{1}{2\sqrt{H}\sqrt{H-y}}. \quad (15)$$

Moreover, by referring to (6) and following the procedure outlined in Ref. [5], specifically considering the region  $\Omega' : -m\sqrt{2gH} < p \leq 0$ , where  $p(y) = mv(y)$ , we can obtain the probability density per unit momentum:

$$\rho_{cl}(p) = \frac{1}{m\sqrt{2gH}}. \quad (16)$$

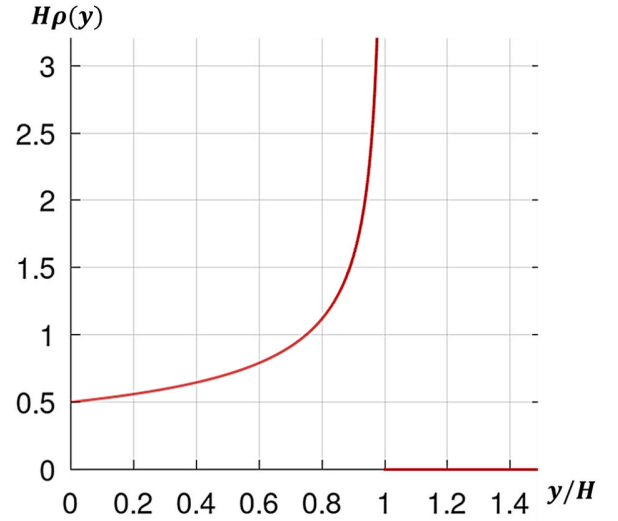


FIGURE 2. Graph illustrating the behavior of the classical probability density per unit length as the height approaches the critical value  $H$ .

Observing the obtained probability density per unit momentum, we note that it exhibits a constant flat behavior. To provide further clarification on this result, Ref. [5] offers an interesting graphical projection technique.<sup>iii</sup>

Figure 2 depicts a strictly increasing curve resembling a “half-parable” shape for the probability density per unit length. The probability density diverges near  $H$  and remains zero above the initial height.

Drawing<sup>iv</sup> on this reasoning, it can be intuited that the probability of finding the particle in the upper half of the falling space is greater than the probability of locating it in the lower half. To verify this, we resort to (5) for each of the aforementioned regions:

$$P(0 < y \leq H/2) = \frac{2 - \sqrt{2}}{2}, \quad (17)$$

$$P(H/2 < y \leq H) = \frac{\sqrt{2}}{2}. \quad (18)$$

Furthermore, the expected values of the position and momentum are calculated using (7) and (8), respectively:

$$\langle y_{cl} \rangle = \frac{2H}{3}. \quad (19)$$

It is noteworthy that the calculated average value for the position of the particle lies above the midpoint of the trajectory, specifically exceeding  $H/2$ . This observation aligns with the intuition that the particle spends more time in that region of the trajectory. Similarly, the average value of momentum  $p$  is also determined:

$$\langle p_{cl} \rangle = \frac{mv_{\max}}{2}. \quad (20)$$

The obtained results, as shown above, are independent of the object's mass (except for the probability density per unit momentum), which agree with the expected behavior based on

the weak equivalence principle. This principle establishes an equivalence between the inertial mass and the passive gravitational mass of the particle. It is important to note the distinction between passive gravitational mass, which measures the gravitational force acting on a body in a given gravitational field, and active gravitational mass, which measures the strength of a body as a source of gravitational field [8].

To experimentally verify the weak equivalence principle with significant accuracy, a series of experiments known as Eötvös experiments have been conducted. These experiments involve a torsion balance comprising two different materials at each end, subject to ideal conditions to minimize temperature gradients and air currents [8]. However, earlier tests by Newton, Galileo, and Bessel employed pendulums with less precision compared to the Eötvös experiments [9]. Over time, these test experiments have been refined, with the most recent being the MICROSCOPE mission. The MICROSCOPE mission utilizes a mechanism with two successive differential accelerometers, achieving higher accuracy than its predecessors [10].

## 5. Relativistic Case

Consider a particle with relativistic mass  $m$  undergoing free fall under the same initial conditions as classical free fall. However, in this scenario, the particle requires an initial height  $H$  that is sufficiently large to attain relativistic speeds, approaching the speed of light in a vacuum denoted as  $c$ . The experimental conditions ensure that the particle's motion is constrained to the vertical direction, with the only force acting on it being gravitational:

$$\mathbf{F} = m\mathbf{g}, \quad (21)$$

Defining the relativistic mass of the particle as  $m = \gamma m_0$ , where  $\gamma = [1 - (v/c)^2]^{-1/2}$  represents the Lorentz factor and  $m_0$  denotes the rest mass. To incorporate the effects of relativity, we employ the relativistic form of Newton's second law as derived in the Ref. [11]:

$$m\mathbf{a} = \mathbf{F} - \frac{(\mathbf{F} \cdot \mathbf{v})}{c^2} \mathbf{v}. \quad (22)$$

By solving the resulting differential equation in the direction of the gravitational field, incorporating the substitution of (21) into (22), and taking into account the initial conditions stated in (9), we can derive the kinematic equations for velocity  $v(t)$  and position  $y(t)$ :

$$v(t) = -c \tanh\left(\frac{gt}{c}\right), \quad (23)$$

$$y(t) = H - \frac{c^2}{g} \ln\left(\cosh\left[\frac{gt}{c}\right]\right). \quad (24)$$

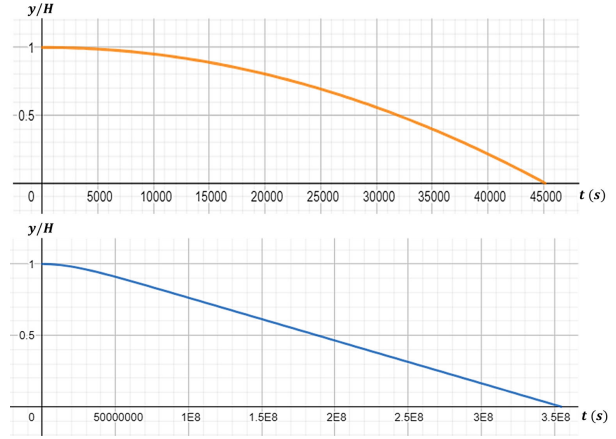


FIGURE 3. Graphics showing the comparison of the position behavior between classical approximation (orange line) and relativistic case (blue line).

The verification of the approximation to classical kinematic expressions can be accomplished by utilizing the Taylor series expansions presented in (A.2) and (A.3), along with condition (29).

By employing the derived kinematic equations for velocity (23) and position (24), we can determine the total fall time  $T_{\text{rel}}$ :

$$T_{\text{rel}} = \frac{c}{g} \text{arc cosh} [\exp(\alpha)], \quad (25)$$

where we introduce the parameter  $\alpha = gH/c^2$ . This dimensionless parameter is useful to analyze the system's behavior, allowing us to study its characteristics based on the relative magnitude of  $\alpha$ .

To facilitate the analysis, it is advantageous to express velocity in terms of position. By combining the expressions for (23) and (24), we obtain:

$$v(y) = -c \sqrt{1 - \exp\left[\frac{2g(y-H)}{c^2}\right]}. \quad (26)$$

Following this expression, we obtain the relativistic momentum [12], in terms of  $y$ :

$$p(y) = -m_0 c \sqrt{\exp\left[\frac{2g(H-y)}{c^2}\right] - 1}. \quad (27)$$

By substituting (25) and (26) into (2), we can derive the expression for the probability density per unit length in the relativistic case as follows:

$$\rho_{\text{rel}}(y) = \frac{g}{c^2 \text{arc cosh} [\exp(\alpha)] \sqrt{1 - \exp\left[\frac{2g(y-H)}{c^2}\right]}}, \quad (28)$$

It is reasonable to consider that these results closely resemble the classical case when the fall time  $T_{\text{rel}}$  or initial height  $H$  are sufficiently small. The key question is how small these quantities need to be in comparison to the other involved constants  $g$  and  $c$ .

To investigate the classical approximation, we observe that the time  $t$  must satisfy the following condition:

$$\frac{gt}{c} \ll 1. \quad (29)$$

This guarantees that the particle moves at very small velocities compared to  $c$ , just as it happens for the classical case.

In the same way,  $H$  must satisfy the condition of being small enough compared to  $g/c^2$ , such that the particle has sufficiently small fall times, and consequently its maximum speed at the instant it reaches the ground, remains small compared to  $c$ , consequently:

$$\alpha \rightarrow 0. \quad (30)$$

It is worth noting that when the initial heights are significantly larger than  $g/c^2$ , we can deduce that:

$$e^\alpha \gg 1. \quad (31)$$

This condition implies that the speeds under consideration are extremely close to the limit of the speed of light  $c$ .

When analyzing the system in the limit of low speeds, as indicated by condition (30), the probability density behavior in the relativistic case approximates that of the classical case. This approximation can be analytically verified by utilizing the results obtained from the Taylor series expansions shown in (A.1), (A.3), and (A.4).

These results enable us to derive the classical approximation for both the total fall time  $T_{(A.1)}$  and the velocity  $v(y)$ , as showed below:

$$T_{\text{rel}} \approx \sqrt{\frac{2H}{g}} = T_{\text{cl}}, \quad (32)$$

$$v(y) \approx -\sqrt{2g(H-y)}. \quad (33)$$

Replacing in (2) verifies the classical approximation:

$$\rho_{\text{rel}}(y) \approx \frac{1}{2\sqrt{H}\sqrt{H-y}} = \rho_{\text{cl}}(y), \quad (34)$$

Figure 4 illustrates the behavior of the probability density per unit length in the relativistic case for different values of  $\alpha$ . As  $\alpha \rightarrow 0$ , the probability density approximates the classical case shown in Fig. 2, providing graphical confirmation of the approximation (34). On the other hand, as  $\alpha$  increases towards larger values, corresponding to speeds close to the speed of light  $c$ , the probability density exhibits a distinct behavior. It resembles that of a particle moving at a constant velocity along a straight trajectory of length  $H$ . Notably, the probability density sharply tends towards infinity when approaching a point near  $H$  from the left.

Figure 4 also reveals an interesting observation for a particle with a velocity close to  $c$ . The probability  $P(0 < y \leq H/2)$  is nearly equal to  $P(H/2 < y \leq H)$  which approximates to  $1/2$ , being slightly higher the probability value in the upper region, as anticipated in the previous case.

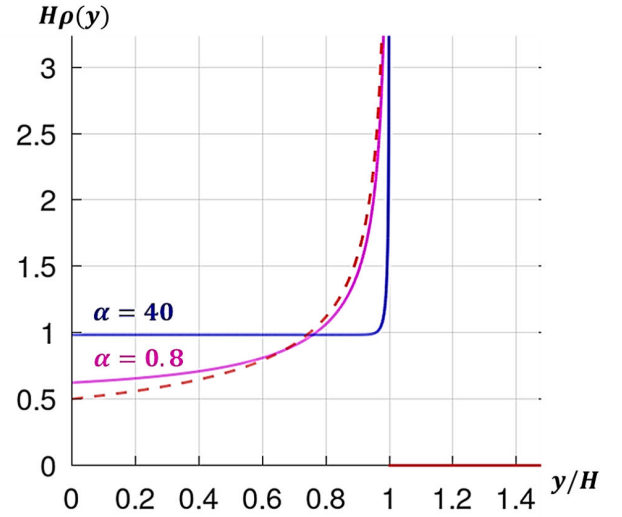


FIGURE 4. Graph for the relativistic probability density per unit length. The blue line corresponds to the case of velocities close to  $c$ . The magenta line to the case of small velocities compared with  $c$ . As can be seen, this one approaches to the classical case (red dashed line).

Regarding the expected values of position and momentum, we can derive them for the relativistic case using (7) and (8). Specifically, we start with the expression for  $\langle y_{\text{rel}} \rangle$  deduced in (C.6), which yields:

$$\langle y_{\text{rel}} \rangle = H \lim_{n \rightarrow \infty} \left[ \frac{1}{2n} + \frac{\xi(\alpha, n)}{n} \right], \quad (35)$$

where the function  $\xi(\alpha, n)$  is expressed as:

$$\xi(\alpha, n) = \sum_{j=1}^{n-1} \frac{\text{arc cosh}[\exp(\alpha j/n)]}{\text{arc cosh}[\exp(\alpha)]}. \quad (36)$$

To compute  $\langle y_{\text{rel}} \rangle$ , we employed the composite trapezoidal rule from (B.5). Subsequently, by starting from (35), we can deduce the limit when the particle moves at speeds very close to  $c$ . By applying L'Hôpital's rule to (36) under the condition (31), we obtain the following expression:

$$\xi(n) \approx \frac{1}{n} \sum_{j=1}^{n-1} j = \frac{(n-1)}{2}, \quad (37)$$

and consequently, it is obtained:

$$\langle y_{\text{rel}} \rangle \rightarrow \frac{H}{2}. \quad (38)$$

Likewise, in the case of velocities that are small compared to  $c$ , we once again apply L'Hôpital's rule under the condition (30), resulting in the expression for  $\xi(n)$  as follows:

$$\xi(n) \approx \frac{1}{n^{1/2}} \sum_{j=1}^{n-1} j^{1/2} = \frac{H_{-1/2}(n-1)}{n^{1/2}}, \quad (39)$$

where  $H_{-1/2}(n-1)$  is the generalized harmonic number of order  $n-1$  of  $-1/2$  represented in (D.7). Obtaining thus the classical approximation by resorting (D.10):

$$\langle y_{rel} \rangle \approx \frac{2H}{3} = \langle y_{cl} \rangle. \quad (40)$$

Furthermore, by considering  $\Omega'$ :  $-m_0c[\exp(2\alpha) - 1]^{1/2} < p \leq 0$ , we calculate the probability density per unit momentum for the relativistic case using a similar procedure as described in the previous case and detailed in Ref. [5]. This involves utilizing (6) and substituting the expression of the relativistic momentum from (27):

$$\rho_{rel}(p) = \frac{1}{\text{arc cosh}[\exp(\alpha)] \sqrt{(m_0c)^2 + p^2}}. \quad (41)$$

This result is slightly more complex compared to its classical counterpart, as the probability density in the relativistic case is not constant as in the previous case. Moreover, it reaches its maximum value when  $p = 0$ , which corresponds to the particle being at the initial point of the trajectory at  $y = H$ . In the limit of low speeds, where  $p \ll m_0c$  and  $\sqrt{(m_0c)^2 + p^2} \approx m_0c$ , we obtain the classical approximation for this probability density by referring to (25) and (32):

$$\rho_{rel}(p) \approx \frac{1}{m_0\sqrt{2gH}} = \rho_{cl}(p). \quad (42)$$

Meanwhile, by utilizing (8) and (37), we can determine the average value of the relativistic momentum in the relativistic case as follows:

$$\langle p_{rel} \rangle = \frac{-m_0c[\exp(\alpha) - 1]}{\text{arc cosh}[\exp(\alpha)]}. \quad (43)$$

It is important to observe that in the case of velocities very close to  $c$ , the average value  $\langle p_{rel} \rangle$  exhibits a divergent behavior of order  $O(\exp(\alpha)/\alpha)$  around values of  $\alpha$  that satisfy the condition (31).

On the other hand, in the case of small velocities compared to  $c$ , where  $\alpha$  satisfies the condition (30), we can observe the classical approximation by considering (25), (32), and (A.4):

$$\langle p_{rel} \rangle \approx \frac{m_0v_{\max}}{2} = \langle p_{cl} \rangle, \quad (44)$$

Additionally, it is important to note that the behavior of the particle in this context is purely kinematic, which means that the probability differential  $dP$  is independent of the relativistic mass and does not depend on the particle's own mass either. As in the classical case, it is important to note that this analysis does not serve as a proof or verification of the weak equivalence principle. However, the fact that the motion exhibits these characteristics aligns with the flat geometry inherent to Minkowski space, upon which Special Relativity is built upon [13].

Given the preceding discussion, one might question the validity of the obtained results for free fall in the framework

of Special Relativity, considering the inclusion of gravitational fields inherent in such an analysis. Therefore, it is essential to clarify that Special Relativity serves as an approximation to General Relativity specifically when dealing with weak gravitational fields [13].

## 6. Quantum case

Let's consider a particle under the influence of a gravitational field. In this scenario, the potential can be defined as follows:<sup>v</sup>

$$V(y) = \begin{cases} mgy, & y \geq 0 \\ \infty, & y < 0 \end{cases}. \quad (45)$$

Such particle is considered to be confined within the region defined by  $\Omega$ :  $0 < y < \infty$ .

Taking into consideration the time-independent Schrödinger equation provided in Ref. [16] and replacing the potential given in (45), we have that:

$$E\psi = -\frac{\hbar^2}{2m} \frac{\partial^2 \psi}{\partial y^2} + mgy\psi. \quad (46)$$

Upon solving the differential equation as shown in Ref. [17], we obtain the eigenfunctions solution:

$$\psi_n(y) = A \left( Ai \left[ \frac{1}{l_g} \left\{ y - \frac{E}{mg} \right\} \right] \right), \quad (47)$$

where the Airy function is denoted as  $Ai^{vi}$  and the principal quantum number of the particle is denoted as  $n$ . The length  $l_g$ , defined as  $l_g = (\hbar^2/2m^2g)^{1/3}$ , is referred to as the "gravitational length" or "characteristic length" [18]. This length has significant value specifically for objects with very small mass. For instance, in the case of the Hydrogen atom,  $l_g = 5.87 \mu\text{m}$ , and for lighter particles such as the electron,  $l_g = 0.88 \text{ mm}$ .

According to the boundary condition for the wave function given by  $\psi_n(0) = 0$ , considering the ground as a reflecting surface <sup>vii</sup>, we can obtain the energy eigenvalues of the particle as  $E_n = -mgl_g a_n$  when  $a_n$  represents the  $n$ -th zero of the Airy function. Notably, the zeros of the Airy function are quantized, confirming the quantization of the energy spectrum. Denoting  $-l_g a_n = H_n$  as the quantized heights of fall of the object, the energy can be expressed as  $E_n = mgH_n$ . Then, we can rewrite (47) in a simplified form:

$$\psi_n(y) = A \left( Ai \left[ \frac{y}{l_g} + a_n \right] \right), \quad (48)$$

and by means of the normalizing condition:

$$A^2 \left( \int_0^\infty Ai^2 \left[ \frac{y}{l_g} + a_n \right] dy \right) = 1, \quad (49)$$

Computing the integral by using (E.13) and solving for  $A$ , we have that:

$$\psi_n(y) = \frac{1}{\sqrt{l_g}} \frac{Ai\left(\frac{y}{l_g} + a_n\right)}{Ai'(a_n)}. \quad (50)$$

We can also express the probability density per unit length associated with the particle as:

$$\rho_n^{qm}(y) = \left[ \frac{1}{\sqrt{l_g}} \frac{Ai\left(\frac{y}{l_g} + a_n\right)}{Ai'(a_n)} \right]^2, \quad (51)$$

Unlike the previous cases, this probability density does not vanish for position values above  $H_n$ . Then, we can get the probability for finding the particle in such region by resorting (E.14), thus:

$$P(y > H_n) = \int_{H_n}^{\infty} \rho_n^{qm}(y) dy = \left[ \frac{Ai'(0)}{Ai'(a_n)} \right]^2, \quad (52)$$

It can also be observed through differentiation that the probability density decreases for  $y > H_n$ . As a result, we can anticipate an evanescent behavior of the wave function as we move away from  $H_n$ . This behavior is supported by the properties of the Airy functions given in (E.16) and (E.17), where both  $Ai(y)$  and  $Ai'(y)$  tend to zero as  $y \rightarrow \infty$ . Consequently, the probability density also tends to zero. In the asymptotic case, as expressed in (E.17), it can be verified that  $Ai'^2(a_n) \approx \sqrt{-a_n}/\pi$  for  $n \gg 1$ . Thus, it is evident that the probability (52) approaches this value in the asymptotic regime:

$$P(y > H_n) \approx \frac{\gamma}{\sqrt{-a_n}}. \quad (53)$$

Here, we have  $\gamma = \pi Ai'^2(0) \approx 0.21$ . Consequently, it can be observed that as  $n$  increases, the probability given by (53) decreases. In the case where  $n \gg 1$ , the probability approaches zero, a result predicted by Classical Mechanics.

When analyzing the probability density corresponding to the quantum case, we can also verify the classical approximation for this result. However, the process for verifying this approximation in the current case is more complex than the relativistic case. According to the methodology outlined in Ref. [19], which demonstrates its application to the particle in a box and the harmonic oscillator problems, the probability density can be transformed into momentum space using a Fourier transform. This transformation allows for the application of a correspondence principle, which extends the Bohr-Heisenberg principle. The effectiveness of this method has also been demonstrated in the study conducted in Ref. [20], where it was successfully applied to the quantum analogue of Kepler's problem.

Regardless, in the specific case we are considering, performing the calculation using standard integration techniques is not feasible since the result cannot be expressed in terms of elementary functions. Therefore, we resort to Albright's method provided in Ref. [21], which is explained in more detail in Refs. [14, 15], to obtain the Fourier transform:

$$\rho_n^{qm}(p) \approx \frac{e^{-iQ}}{2\pi\hbar} \sqrt{\frac{\pi}{2Q}} \left[ C \left( \sqrt{\frac{2Q}{\pi}} \right) + iS \left( \sqrt{\frac{2Q}{\pi}} \right) \right] + \rho_n^{(1)}(p), \quad (54)$$

Let  $Q \equiv pH_n/\hbar$ . Additionally,  $C(x)$  and  $S(x)$  represent the Fresnel integrals [22]. It is important to note that there exists a first-order correction term in the approximation denoted as  $\rho_n^{(1)}(p)$ , whose expression is provided in Ref. [15]. This correction term can be expressed as a power series, given by the following:

$$\rho_n^{(1)}(p) = \frac{e^{-iQ}}{4\pi\hbar a_n^3} \sum_{j=0}^{\infty} \left[ \frac{(-iQ)^j j(j-1)(j-2)}{j!(2j+1)(2j-5)} \right], \quad (55)$$

On the other hand, the quotient between Planck's constant and the classical action can be calculated. The result is

$$\frac{\hbar}{S_{cl}} = \frac{\hbar}{mgH\sqrt{\frac{2H}{g}}} = \frac{\hbar}{\sqrt{2m^2gH^3}}.$$

Furthermore, for  $n \gg 1$ , it is satisfied that

$$\frac{1}{a_n^{3/2}} = \frac{\hbar}{\sqrt{2m^2gH^3}}.$$

Analyzing the correction term (55), it can be verified that this is a quadratic order term in the quotient of the Planck's constant and the classical action:

$$\rho_n^{(1)}(p) \sim O\left(\frac{1}{a_n^3}\right) = O\left(\frac{\hbar}{S_{cl}}\right)^2, \quad (56)$$

Observe that this quotient depends on the mass of the particle, raising the possibility that the weak equivalence principle could be violated in the quantum case of free fall.

Then, by calculating the inverse Fourier transform for the first term (54), the classical approximation for the probability density is obtained, as shown in Refs. [14, 15], under the condition  $n \gg 1$  and therefore  $H_n \rightarrow H$ , where  $H$  represents the classical height:

$$\rho_n^{qm}(y) \sim \frac{1}{2\sqrt{H}\sqrt{H-y}} = \rho_{cl}(y), \quad (57)$$

The second term of the approximation must provide quantum corrections at the macroscopic level:

$$\rho_n^{(1)}(y) = \frac{1}{2\pi\hbar} \int_0^{\infty} \rho_n^{(1)}(p) e^{\frac{ipy}{\hbar}} dp, \quad (58)$$

This integral cannot be easily calculated, but numerical approximations can be made.

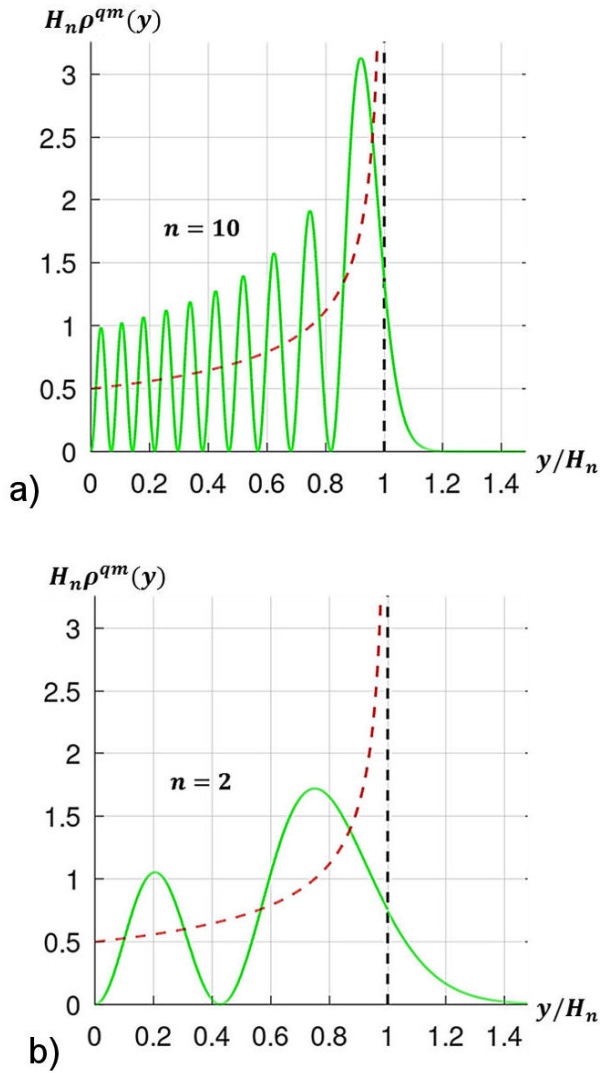


FIGURE 5. Graph for the quantum probability density (green line) and classical probability density (red dashed line), for the case of  $n = 2$  (bottom) and the case of  $n = 10$  (top). Turning point is represented with the black dashed line.

Figure 5 illustrates the classical and quantum probability density graphs for the cases with  $n = 2$  and  $n = 10$ . It can be observed that as  $n$  increases, the quantum probability density becomes more similar to the classical probability density on average. Moreover, it is noted that the quantum probability density  $\rho_n^{qm}(y)$  exponentially decays beyond the height  $H_n$ . While the probability of finding the particle above  $H_n$  is not zero, the exponential decay becomes more pronounced with larger values of  $n$ , eventually recovering the expected behavior of the classical case. In the classical case, it can be crudely stated that “particles do not fall upwards” in contrast to the quantum case studied.

In addition to the theory proposed by Ref. [14], this work analyzes the expected values of position and momentum observables in the quantum case, calculated using the following expressions [23]:

$$\langle y_{qm} \rangle = \int_{\Omega} y \psi_n^*(y) \psi_n(y) dy, \quad (59)$$

$$\langle p_{qm} \rangle = -i\hbar \int_{\Omega} \psi_n^*(y) \frac{\partial}{\partial y} \psi_n(y) dy, \quad (60)$$

The expected value of the position can be calculated using (59). To obtain this value, we apply integration by parts, utilizing Albright’s method. The result of this calculation is shown in (E.15). By evaluating this expression in the appropriate region, we obtain the following result:

$$\langle y_{qm} \rangle = \frac{2H_n}{3}. \quad (61)$$

As mentioned earlier, in the limit of high energies, the height  $H_n$  approaches the classical height  $H$ , leading to the classical approach:

$$\langle y_{qm} \rangle \approx \frac{2H}{3} = \langle y_{cl} \rangle. \quad (62)$$

Using (60) and resorting (E.14), the expected value of the momentum is calculated as:

$$\langle p_{qm} \rangle = 0, \quad (63)$$

The average value of the momentum implies that it can point both away from the surface and towards it. Additionally, the result (63) can be easily obtained using Ehrenfest’s theorem. By applying the theorem, we find that since  $\langle y_{qm} \rangle$  is independent of time, its time derivative is zero, leading to

$$\frac{\langle p_{qm} \rangle}{m} = \frac{d \langle y_{qm} \rangle}{dt} = 0.$$

It is worth noting that Ehrenfest’s theorem is applicable in this particular case, as the force applied on the particle is constant [24]. These results align with the findings of Ref. [25], which provides a more detailed calculation of the expected values in the quantum case, including higher-order terms.

As stated in Ref. [15], the expected values obtained for each of these physical observables should closely approximate their corresponding values in Classical Mechanics. The article outlines a systematic approach for determining the classical limit of periodic quantum systems, and demonstrates its successful application to the quantum bouncer problem. It is important to note that in this discussion, the classical problem of the rebounding particle (bouncer) is assumed as the correct classical approximation for the quantum case. However, in the present work, as mentioned before, the classical analysis is limited to considering only the trajectory of the falling particle, excluding the subsequent rebound.



FIGURE 6. Diagram illustrating the relationship between the three theories. The arrows represent the connections between them, showcasing the role of probability density  $\rho(y)$  in bridging them.

## 7. Conclusions

It can be observed that, in general, the probability densities for the relativistic and quantum cases differ from those obtained in the classical case. However, in the second and third cases, the probability densities closely approximate the classical result when the speed is much less than the speed of light in a vacuum and when the actions are much greater than the value of Planck's constant, respectively. Similarly, the expected values of position and momentum observables in the relativistic and quantum theories approximate those found in the classical case. Therefore, the probability density serves as a connection between these three different theories, despite being expressed differently. This relationship is illustrated in Fig. 6.

The discussion on the validity of the weak equivalence principle in each theory examined in this paper was briefly touched upon from a non-rigorous perspective. Additionally, a more in-depth analysis is required for the quantum theory, and it is suggested that future works consider calculating higher-order quantum corrections for the probability density, as well as the corresponding inverse Fourier transform.

This work holds pedagogical value in comparing and discussing the phenomenon of free fall across Classical Mechanics, Relativistic Mechanics, and Quantum Mechanics using the concept of probability density.

The approach presented in this work also introduces a variety of mathematical methods for analyzing and understanding the phenomenon from each theory aforementioned.

One of these methods is the graphical projection technique, as detailed in Ref. [5], which involves sketching probability density graphics based on known position and velocity graphics. This technique allows students to visually represent the probability distribution associated with the system and explore the probabilistic nature of other mechanical phenomena.

Taylor series expansions are a fundamental mathematical technique widely employed in Physics to approximate and investigate diverse functions. These expansions play a crucial role in examining systems near equilibrium or in specific scenarios, such as analyzing the thermodynamics of a system at low temperatures or studying the electromagnetic properties of a particle by expanding the electrostatic potential around a particular point. In our research, we applied Taylor series expansions to analyze the relativistic case at low velocities, providing insights into the classical limit of the system.

Additionally, we discovered an uncommon application of generalized harmonic numbers in Physics. The aforementioned application was supported by deducing its asymptotic expansion through the utilization of the Euler-Maclaurin formula (D.8). This formula is useful in various physical contexts, some examples being calculations of definite integrals, approximation of sums, and the analysis of statistical mechanics systems, such as the computation of some partition functions.<sup>viii</sup>

Moreover, Airy functions and the Albright's method find extensive and diverse applications in Physics, as provided in Ref. [26]. These functions were originally introduced by G.B. Airy for calculating light intensity near caustics in Optics. They also find utility in Fluid Mechanics, particularly in the analysis of stability properties using the Orr-Sommerfeld equation. Furthermore, in Quantum Mechanics, Airy functions are used in the computation of the one-dimensional Wigner semiclassical distribution.

The method outlined in Ref. [19] offers students a systematic approach to verify the convergence of Quantum Mechanics to Classical Mechanics in the high-energy asymptotic regime, as predicted by the Bohr-Heisenberg correspondence principle. This serves as an invitation for students to delve deeper into the references provided [19, 20] in which this method has been successfully applied and explore additional quantum systems, such as the circular potential well and spherical harmonic oscillator.

Through the application of these methods, students not only develop the ability to analyze the phenomenon of free fall but also acquire valuable skills in solving Physics problems using mathematical techniques. This work encourages students to explore additional physical applications where these mathematical methods can be effectively employed.

It is worth noting that the analysis and discussion of the relativistic case presented in this paper are rarely found in the literature.

## Appendix

### A. Taylor series

The following expansions are used to compute some classical approximations [27]:

$$\cosh(x) = 1 + \frac{x^2}{2} + O(x^4), \quad (\text{A.1})$$

$$\tanh(x) = x + O(x^3), \quad (\text{A.2})$$

$$\ln[\cosh(x)] = \frac{x^2}{2} + O(x^4), \quad (\text{A.3})$$

$$\exp(x) = 1 + x + O(x^2). \quad (\text{A.4})$$

## B. Composite trapezoidal rule

When grid spacing is uniform, the approximation integral is given by [28]:

$$\int_a^b f(x) dx \approx \frac{b-a}{n} \left[ \frac{f(a)+f(b)}{2} + \sum_{j=1}^{n-1} f\left(a + j \frac{b-a}{n}\right) \right]. \quad (\text{B.1})$$

## C. Deduction of $\langle y_{rel} \rangle$

$$\langle y_{rel} \rangle = \frac{g}{c^2} \int_0^H \frac{y dy}{\text{arccosh}[\exp(\alpha)] \sqrt{1 - \exp\left(\frac{2g(y-H)}{c^2}\right)}},$$

Integrating by parts [27]:

$$\langle y_{rel} \rangle = - \frac{y \text{ arc cosh}[\exp(\frac{g(H-y)}{c^2})]}{\text{arc cosh}[\exp(\alpha)]} \Big|_0^H + \int_0^H \frac{\text{arc cosh}[\exp(\frac{g(H-y)}{c^2})]}{\text{arc cosh}[\exp(\alpha)]} dy,$$

Notice that the first term vanishes. Then, let the substitution  $u = 1 - (y/H)$ , so we have:

$$\langle y_{rel} \rangle = H \int_0^1 \frac{\text{arc cosh}[\exp(\alpha u)]}{\text{arc cosh}[\exp(\alpha)]} du, \quad (\text{C.1})$$

## D. Generalized harmonic number

The generalized harmonic number can be expressed by the following sum [29]:

$$H_m(n) = \sum_{j=1}^n j^{-m}. \quad (\text{D.1})$$

To showcase the expansion of the generalized harmonic number, we can begin by utilizing the Euler-Maclaurin summation formula [30]:

$$\sum_{j=1}^n f(j) = \int_1^n f(x) dx + \frac{1}{2}[f(n) + f(1)] + \sum_{j=1}^{\lfloor p/2 \rfloor} \frac{B_{2j}}{(2j)!} [f^{(2j-1)}(n) - f^{(2j-1)}(1)] + R_p, \quad (\text{D.2})$$

Where  $R_p$  represents a residual term that is typically negligible for appropriate values of  $p$  and  $B_{2j}$  the  $2j$ -th Bernoulli number. By choosing  $f(x) = x^{-m}$ , we obtain the following expression:

$$\begin{aligned} \sum_{j=1}^n j^{-m} &= \int_1^n x^{-m} dx + \frac{1}{2}[n^{-m} + 1^{-m}] \\ &+ \sum_{j=1}^{\lfloor p/2 \rfloor} \frac{B_{2j}}{(2j)!} \left[ (m+1)(m+3) \dots \right. \\ &\dots (m+2j-2)n^{-m-2j+1} \\ &\left. - (m+1)(m+3) \dots (m+2j-2) \right] + R_p. \end{aligned}$$

Simplifying the expression, we get:

$$\begin{aligned} \sum_{j=1}^n j^{-m} &= \frac{1}{1-m} n^{1-m} + \frac{1}{m-1} + \frac{1}{2} + \frac{1}{2} n^{-m} \\ &+ \sum_{j=1}^{\lfloor p/2 \rfloor} \frac{B_{2j}}{(2j)!} \left[ (m+1)(m+3) \dots \right. \\ &\left. \dots (m+2j-2)(n^{-m-2j+1} - 1) \right] + R_p. \end{aligned}$$

These can be expressed asymptotically by consolidating the constants into a single value using the Riemann zeta function, leading to the following form:

$$\begin{aligned} \sum_{j=1}^n j^{-m} &\sim \zeta(m) + \frac{1}{1-m} n^{1-m} + \frac{1}{2} n^{-m} \\ &+ \sum_{j=1}^{\lfloor p/2 \rfloor} \frac{B_{2j}}{(2j)!} \left[ (m+1)(m+3) \dots \right. \\ &\left. \dots (m+2j-2)n^{-m-2j+1} \right]. \end{aligned}$$

By observing the last term, we can conclude that it is of order  $O(n^{-m-1})$ . Consequently, we finally deduce that:

$$\begin{aligned} H_m(n) &= \zeta(m) + \frac{1}{1-m} n^{1-m} \\ &+ \frac{1}{2} n^{-m} + O(n^{-m-1}). \end{aligned} \quad (\text{D.3})$$

In particular, we have that the expansion for  $H_{-1/2}(n)$  is:

$$\begin{aligned} H_{-1/2}(n) &= \zeta\left(-\frac{1}{2}\right) + \frac{2}{3} n^{3/2} \\ &+ \frac{1}{2} n^{1/2} + O(n^{-1/2}), \end{aligned} \quad (\text{D.4})$$

where  $\zeta(-1/2) = 0.2078862250\dots$  is a particular value of the Riemann zeta function [31]. Notably, the mathematician Ramanujan established the expression presented in Equation (D.4) in his work [32], without explicitly indicating the direct involvement of the evaluated Riemann Zeta function in this particular result.

## E. Airy functions and notable results

The Airy's equation [26] appears as:

$$\frac{d^2y}{dx^2} = xy, \quad (\text{E.1})$$

Its general solution is expressed as:

$$y = C_1 Ai(x) + C_2 Bi(x), \quad (\text{E.2})$$

To simplify calculations involving the Airy functions  $Ai(x)$  and  $Bi(x)$ , it is possible to use the Albright's method provided in Ref. [21]. This method allows us to express any linear combination (E.2) as a linear combination of their derivatives. Here, we present the integral results particularly for  $Ai(x)$ :

$$\int Ai^2(x) dx = xAi^2(x) - Ai'^2(x), \quad (\text{E.3})$$

$$\int Ai(x)Ai'(x) dx = \frac{1}{2}Ai^2(x), \quad (\text{E.4})$$

$$\int xAi^2(x) dx = \frac{1}{3}[Ai(x)Ai'(x) - xAi'^2(x) + x^2Ai^2(x)], \quad (\text{E.5})$$

It is also useful to have the following asymptotic approximations [26]:

$$Ai(x) \sim \frac{1}{2\sqrt{\pi}x^{1/4}} e^{-\frac{2}{3}x^{3/2}} \times \left( 1 + \sum_{k=1}^{\infty} \frac{(-1)^k (2k-1)!!}{(2x)^{3k/2}} \right), \quad (\text{E.6})$$

$$Ai'(x) \sim \frac{1}{\sqrt{\pi}} x^{1/4} e^{-\frac{2}{3}x^{3/2}} \times \left( -\frac{1}{2} + \sum_{k=1}^{\infty} \frac{(-1)^k (2k+1)!!}{(2x)^{3k/2+1}} \right), \quad (\text{E.7})$$

Notice that both expressions vanish as  $x \rightarrow \infty$ .

## Acknowledgments

We acknowledge the helpful observations and suggestions provided by Juan A. Cañas Palomeque. The first author also wants to express his gratitude for the valuable contributions of Maria F. Arias Hernández and Luis G. Romero Hernández.

- 
- i.* In such forum, the physicists Luis de la Peña, Ana María Cetto Kramis, Gerardo Carmona Ruiz, Salvador Cruz Jiménez, Pedro Colina Almazán and Alejandro González Sánchez also participated.
  - ii.* In addition, Moshinsky left us a series of notes compiled in Ref. [1].
  - iii.* In this work, we do not provide a detailed explanation of the application of this method. However, we encourage the reader to refer to the mentioned article for a more comprehensive understanding.
  - iv.* The variables of the axis have been selected in a way that the quantities are dimensionless for each graph shown in this work.
  - v.* The theoretical approach of this section has as a fundamental references the pedagogical materials [14, 15].
  - vi.* The other independent solution of the Airy equation  $Bi$ , has been eliminated because it is divergent as  $y \rightarrow \infty$ .
  - vii.* The potential given by (45) indicates that the ground is impenetrable by the particle.
  - viii.* A detailed procedure for applying this formula can be found in Appendix D of this work.
1. E. Chacón, Apuntes del Curso de Mecánica Cuántica de Marcos Moshinsky, 1st ed. (Las Prensas de Ciencias, CDMX, 2008).
  2. N. Wheeler, Classical/Quantum Motion in a Uniform Gravitational Field, <https://www.reed.edu/physics/faculty/wheeler/documents/Quantum20Mechanics/Miscellaneous%20Essays/Quantum%20Bouncer/Bouncer%20Seminar.pdf>. (2003).
  3. N. Bohr, The Correspondence Principle (North Holland, Amsterdam, 2013).
  4. G. Galilei, Dialogues Concerning Two New Sciences (The Macmillan Company, NY, 1914).
  5. R. Robinett, Quantum and classical probability distributions for position and momentum, *Am. J. Phys.* **63** (1995) 823, <https://doi.org/10.1119/1.17807>.
  6. A. Kolmogorov, Foundations of the Theory of Probability, 2nd ed. (Dover Publications, Mineola, NY, 2013), p. 37, [https://www.york.ac.uk/depts/maths/histstat/kolmogorov\\_foundations.pdf](https://www.york.ac.uk/depts/maths/histstat/kolmogorov_foundations.pdf).
  7. R. Resnick, D. Haliday, and K. Krane, *Physics* **Vol. 1**, 4th ed. (Wiley, Hoboken, NJ, 1991), p. 28.
  8. P. Roll, R. Krotkov, and R. Dicke, The equivalence of inertial and passive gravitational mass, *Ann. Phys.* **26** (1964) 442, [https://doi.org/10.1016/0003-4916\(64\)90259-3](https://doi.org/10.1016/0003-4916(64)90259-3).
  9. I. Ciufolini and J. Wheeler, *Gravitation and Inertia* (Princeton University, NJ, 1995), pp. 117-119.
  10. P. Brax, Satellite Confirms the Principle of Falling, *Phys.* **15** (2022) 94, <https://doi.org/10.1103/Physics.15.94>.
  11. C. Möller, *The Theory of Relativity*, 3rd ed. (Clarendon Press, Oxford, 1952), p. 75.
  12. N. Lemos, *Analytical Mechanics*, 2nd ed. (Cambridge University Press, Cambridge, 2018), p. 200.
  13. G. Naber, *The Geometry of Minkowski Space Time: An Introduction to the Mathematics of the Special Theory of Relativity*, 2nd ed. (Springer, New York, NY, 2011), pp. 1-6.

14. J. Cañas, La Caida Libre Cuántica, Thesis Degree (2019), Universidad Juárez Autónoma de Tabasco.
15. J. Cañas, J. Bernal, and A. Martín-Ruiz, Exact classical limit of the quantum bouncer, *Eur. Phys. J.* **137** (2022) 1310, <https://doi.org/10.1140/epjp/s13360-022-03529-2>
16. N. Zetilli, Quantum Mechanics: Concepts and Applications, 2nd ed. (Wiley, Hoboken, NJ, 2009), p. 179, [https://www.mmmut.ac.in/News\\_content/02110tpnews.11232020.pdf](https://www.mmmut.ac.in/News_content/02110tpnews.11232020.pdf).
17. P. Langhoff, Schrödinger Particle in a Gravitational Well, *Am. J. Phys.* **39** (1971) 954, <https://doi.org/10.1119/1.1986333>.
18. R. Gibbs, The quantum bouncer, *Am. J. Phys.* **43** (1975) 25, <https://doi.org/10.1119/1.10024>.
19. J. Bernal, A. Martín-Ruiz, and J. García Melgarejo, A simple mathematical formulation of the correspondence principle, *J. Mod. Phys.* **4** (2013) 108, <https://doi.org/10.4236/jmp.2013.41017>.
20. A. Martín-Ruiz *et al.*, The Classical Limit of the Quantum Kepler Problem, *J. Mod. Phys.* **4** (2013) 818, <https://doi.org/10.4236/jmp.2013.41017>.
21. J. Albright, Integrals of products of Airy functions, *J. Phys. A: Math. Gen.* **10** (1977) 485, <https://doi.org/10.1119/1.10024>.
22. N. Temme, Error Functions, Dawson's and Fresnel Integrals (Cambridge University Press, Cambridge, 2010).
23. C. Cohen Tannoudji, B. Diu, and F. Laloe, Quantum Mechanics **Vol. 1**, 1st ed. (Wiley, Hoboken, NJ, 1991), p. 229.
24. P. Ehrenfest, Bemerkung uber die angen "aherte g" ultigkeit der klassischen mechanik innerhalb der quantenmechanik, *Z. Phys.* **45** (1927) 455, <https://doi.org/10.1007/BF01329203>.
25. S. Singh, S. Suman, and V. Singh, Quantum-classical correspondence for a particle in a homogeneous field, *Eur. Phys. J.* **37** (2016) 6, <https://doi.org/10.1088/0143-0807/37/6/065405>.
26. M. Vallée, O. Soares, Airy functions and aplications to physics (Imperial College Press, Covent Garden, L, 2004).
27. N. Piskunov, Differential and Integral Calculus (Mir, Moscow, Msk, 1969).
28. J. Burden, R.L. Faires, Numerical Analysis, 9th ed. (Cengage Learning, Boston, MA, 2010), pp. 206-207.
29. J. R. Sousa, Generalized Harmonic Numbers, <https://arxiv.org/abs/1810.07877>.
30. T. Apostol, An Ele (2018)mentary View of Euler's Summation Formula, *Am. Math. Mon.* **106** (1999) 409, <https://doi.org/10.2307/2589145>.
31. M. Anthony, The Towering Zeta Function, *APM.* **6** (2016) 351, <https://doi.org/10.4236/apm.2016.65026>.
32. S. Ramanujan, On the sum of the square roots of the first n natural numbers, *J. Indian Math. Soc.* **7** (1915) 173, <https://ramanujan.sirinudi.org/Volumes/published/ram09.pdf>.